Ultrawideband Radar Time Domain Simulation for the Analysis of Coherent Signal Processing Techniques

Johannes Fink[*]**, Friedrich K. Jondral**[*]
Thomas Bächle[†]**, Oliver Prinz**[†]

[*]Communications Engineering Lab, Karlsruhe Institute of Technology (KIT)
Karlsruhe, Germany
email: {Johannes.Fink, Friedrich.Jondral}@kit.edu

[†]SICK AG
Waldkirch, Germany
email: {Thomas.Baechle, Oliver.Prinz}@sick.de

Abstract: *In this paper a method for performing UWB radar time domain simulations is explained and simulation results are demonstrated. The given results are compared to measurements and the simulation errors are discussed. This constitutes a first step towards development of coherent signal processing techniques for UWB radar.*

1. Introduction

Ultrawideband (UWB) impulse radar uses non-sinusoidal transient signals, which makes time domain analysis a very insightful method to study system behaviour. In this work, a simulation model based on time-domain processing for UWB impulse radar is presented and validated with measurements. This model is applicable to the analysis of coherent signal processing techniques, such as e.g. correlation receiving.

2. System Model

Considering a bistatic impulse radiating UWB radar, which illuminates a stationary target, the methods of linear system theory and the concept of power waves [1] allow modeling the time domain radar link in terms of impulse responses (IRs) as explained in [2]. To account for both co- and cross-polarization, a matrix-vector notation as in [2] is introduced. The transmitted and received signals are modeled as two-element-vectors

$$\mathbf{u}(t) = \left(\begin{array}{c} u^{\mathrm{h}}(t) \\ u^{\mathrm{v}}(t) \end{array} \right), \tag{1}$$

where the first element is the horizontally polarized component and the second the vertically polarized component of the signal. This is denoted by the superscripts h and v, respectively.

Furthermore, each functional block in the transmission chain is modeled using a 2×2 matrix, where each element represents one specific polarization coupling:

$$\mathbf{h}(t, \theta, \phi) = \left[\begin{array}{cc} h^{\mathrm{hh}}(t, \theta, \phi) & h^{\mathrm{hv}}(t, \theta, \phi) \\ h^{\mathrm{vh}}(t, \theta, \phi) & h^{\mathrm{vv}}(t, \theta, \phi) \end{array} \right]. \tag{2}$$

The first letter in the superscripts denotes the polarization of the originating field, the second that of the receiving site. The angles θ and ϕ are the angles in azimuth and elevation, respectively.

With this notation and $(\cdot)^T$ denoting the matrix transpose, the UWB radar link in time domain can be modeled as

$$\mathbf{u}_{\mathrm{rx}}(t) = \frac{1}{2\pi c} \frac{\sqrt{Z_{\mathrm{rx}}}}{\sqrt{Z_{\mathrm{tx}}}} \mathbf{h}_{\mathrm{rx}}^T(t, \theta_{\mathrm{rx}}, \phi_{\mathrm{rx}}) * \left[\mathbf{h}_{\mathrm{cpl}}(t) + \mathbf{h}_{\mathrm{cr}}(t) * \mathbf{h}_{\mathrm{sc}}(t, \theta_{\mathrm{i}}, \phi_{\mathrm{i}}, \theta_{\mathrm{s}}, \phi_{\mathrm{s}}) * \mathbf{h}_{\mathrm{cf}}(t) \right]$$

$$* \mathbf{h}_{\mathrm{tx}}(t, \theta_{\mathrm{tx}}, \phi_{\mathrm{tx}}) * \frac{\partial}{\partial t} \mathbf{u}_{\mathrm{tx}}(t) + \mathbf{n}(t) \tag{3}$$

with $*$ denoting the convolution operation, which is defined for matrices analogous to matrix multiplication. The voltage signal at the receiving antenna ports is $\mathbf{u}_{\mathrm{rx}}(t)$ and the generator signal at the input of the transmit antenna is $\mathbf{u}_{\mathrm{tx}}(t)$. The impedances at the antenna ports Z_{rx} and Z_{tx} are assumed to be frequency independent and equal for both polarizations. The derivation results from the reciprocity theorem [3, 4, 5] and c is the speed of light. The IRs of transmit and receive antenna are $\mathbf{h}_{\mathrm{tx}}(t, \theta_{\mathrm{tx}}, \phi_{\mathrm{tx}})$ and $\mathbf{h}_{\mathrm{rx}}(t, \theta_{\mathrm{rx}}, \phi_{\mathrm{rx}})$, the IRs of forward and return channel are $\mathbf{h}_{cf}(t)$ and $\mathbf{h}_{cr}(t)$ and the IR of the target is $\mathbf{h}_{\mathrm{sc}}(t, \theta_{\mathrm{i}}, \phi_{\mathrm{i}}, \theta_{\mathrm{s}}, \phi_{\mathrm{s}})$. Furthermore, $\mathbf{h}_{\mathrm{cpl}}(t)$ represents the transmitter-receiver coupling and $\mathbf{n}(t)$ is the additive noise term. To account for the angular dependencies, the following angles have been defined:

- main beam angle of transmit antenna: $\theta_{\mathrm{tx}}, \phi_{\mathrm{tx}}$,

- incident angle on target: $\theta_{\mathrm{i}}, \phi_{\mathrm{i}}$,

- scattering angle from target: $\theta_{\mathrm{s}}, \phi_{\mathrm{s}}$,

- incident angle on receive antenna: $\theta_{\mathrm{rx}}, \phi_{\mathrm{rx}}$.

The model along with the used nomenclature is depicted in Fig. 1.

To evaluate (3), the coupling signal $\mathbf{h}_{\mathrm{cpl}}(t)$ is assumed to be stationary and thus can be estimated using an experimental setup in the absence of a target and averaging over a large number of measurements. The assumption of stationarity holds as long as temperature stays constant and direct current drift is suppressed. The antenna IRs $\mathbf{h}_{\mathrm{tx}}(t, \theta_{\mathrm{tx}}, \phi_{\mathrm{tx}})$ and $\mathbf{h}_{\mathrm{rx}}(t, \theta_{\mathrm{rx}}, \phi_{\mathrm{rx}})$ are derived by inverse Fourier transform from transfer functions measured in an anechoic chamber. To assure that the channel can be modeled as single path line-of-sight free space, the measurement is set up such that the next reflecting structure is further away than the distance between
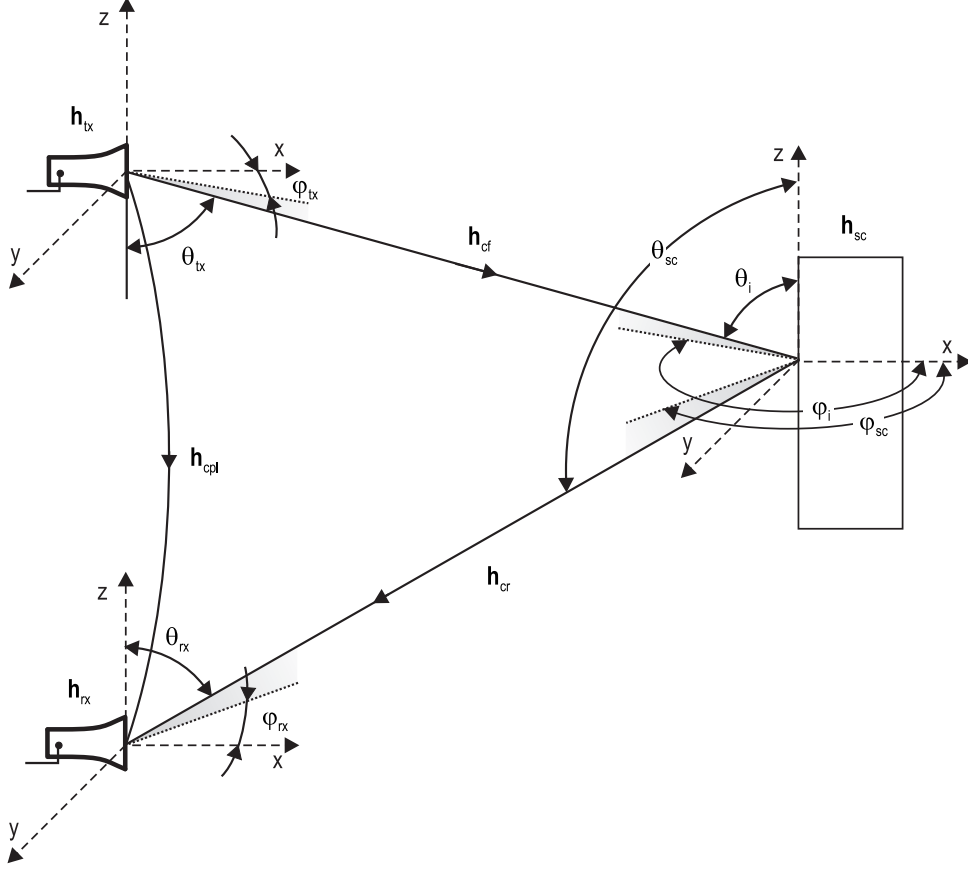
Figure 1: Bistatic full polarimetric system model

target and antenna plus length of the transmitted pulse. Because of a symmetrical measurement geometry, forward and return channel IRs are assumed to be identical

$$\mathbf{h}_{cf}(t) = \mathbf{h}_{cr}(t) = \frac{1}{r+1}\delta\left(t - \frac{r}{c}\right)\begin{bmatrix} 1 & 0 \\ 0 & 1 \end{bmatrix}, \tag{4}$$

where r is the distance between target and antenna and $\delta(\,\cdot\,)$ the dirac delta function to model the delay. The term $\frac{1}{r+1}$ is a modified path loss function to eliminate the singularity at $r = 0$. This modification leads to slight amplitude under-estimation.

Following the procedure above to get the necessary IRs, (3) and (4) can be used together with a given target impulse response $\mathbf{h}_{sc}(t, \theta_i, \phi_i, \theta_s, \phi_s)$ to calculate the expected received signal $\mathbf{u}_{rx}(t)$ for a given generator waveform $\mathbf{u}_{tx}(t)$. This allows analyzing and further processing of these signals.

3. Validation

The model is validated by comparing simulation results for specific target IRs of a flat metal surface and a water surface with measurement results. The IRs are modeled analytically based on electromagnetic scattering theory [6].

The transmitted pulse shape $\mathbf{u}_{\text{tx}}(t)$ used in the simulation has been obtained by measurement from the experimental setup. The horizontal component $u^h_{\text{tx}}(t)$ has been set to 0, as only antennas in vertical polarization have been used. The vertical component $u^v_{\text{tx}}(t)$ is depicted in Fig. 2. Both targets have been illuminated perpendicularly to their surface. Thus, according to [6], the
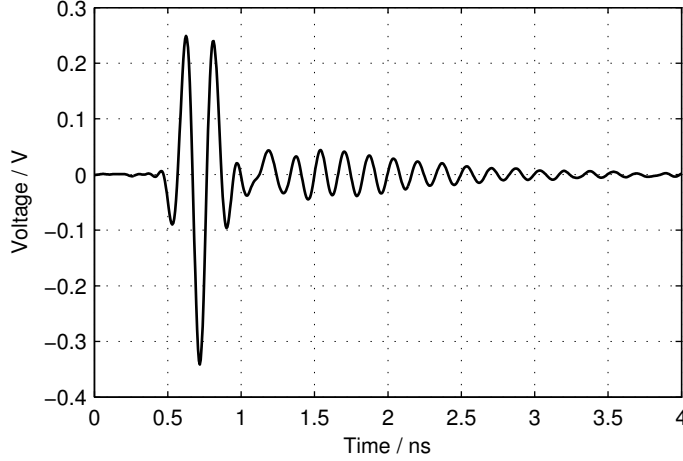

Figure 2: Vertical component of transmitted pulse

scattering transfer function of the metal plate can be modeled as

$$\mathbf{H}_{\text{sc,mp}}(f, 0°, 0°) = 2\sqrt{\pi} A \frac{f}{c_0} \begin{bmatrix} 1 & 0 \\ 0 & 1 \end{bmatrix}, \tag{5}$$

where A is the area of the plate, in our case $0.64\ \text{m}^2$. Inverse Discrete Fourier Transform (IDFT) yields the according impulse response $\mathbf{h}_{\text{sc},mp}(t, 0°, 0°)$.

In order to model the scattering impulse response of the distilled water surface with an area of $0.78\ \text{m}^2$, a result in [7] is used, which states, that at normal incidence, the scattering IR of a dielectric disk $\mathbf{h}_{\text{sc,dd}}(t, 0°, 0°)$ can be modeled as the scattering IR $\mathbf{h}_{\text{sc,mp}}(t, 0°, 0°)$ of a metal disk of same area multiplied by the according reflection coefficient Γ:

$$\mathbf{h}_{\text{sc,dd}}(t, 0°, 0°) = \Gamma\,\mathbf{h}_{\text{sc,md}}(t, 0°, 0°) = \Gamma\,\mathscr{F}^{-1}\left\{\mathbf{H}_{\text{sc,mp}}(f, 0°, 0°)\right\}, \tag{6}$$

where $\mathscr{F}^{-1}\{\cdot\}$ denotes the IDFT. The reflection coefficient at the border of two perfect dielectrics with conductivity zero is

$$\Gamma = \frac{\sqrt{\epsilon_{\text{r,1}}} - \sqrt{\epsilon_{\text{r,2}}}}{\sqrt{\epsilon_{\text{r,1}}} + \sqrt{\epsilon_{\text{r,2}}}}, \tag{7}$$

where $\epsilon_{\text{r,1}}$ and $\epsilon_{\text{r,2}}$ are the permitivities of the first and second dielectric, respectively. The permittivity of air is approximately $\epsilon_r \approx 1$. The frequency dependent permittivity of water can be modeled using the Debye equation [8]

$$\epsilon_{\text{r}} = \epsilon_{\text{r},\infty} + \frac{\epsilon_{\text{r},0} - \epsilon_{\text{r},\infty}}{1 + j\omega\tau}. \tag{8}$$

The values for the necessary material parameters for distilled water can be found in [8] and are summarized in Tab. 1.

To single out the surface reflection in the measurement, a plastic canister filled high enough with distilled water to allow time gating of the surface reflection and thus avoiding problems with late returns from the bottom has been used.

Table 1: Material parameters of distilled water

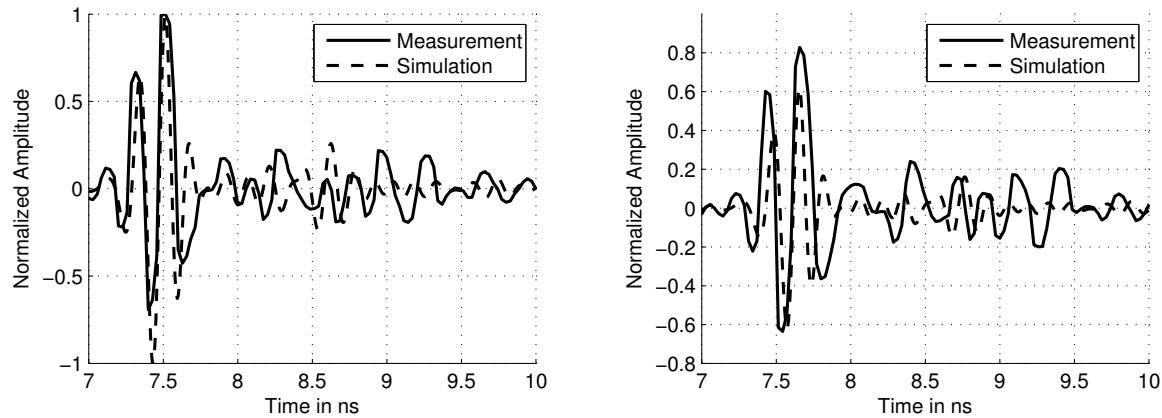| Parameter	Symbol	Value for distilled water
Limit of the relative permittivity at high frequencies	$\epsilon_{r,\infty}$	4.9
Relative permittivity for static fields	$\epsilon_{r,0}$	88.2
Relaxation time	τ	$19.4\,\text{ps}$

The results of both measurements and simulations are depicted in Fig. 3. For the metal plate in Fig. 3a, the actual pulse matches excellently. In the time bins after the main pulse, the amplitude difference matches. The difference between measurement and model can be explained by secondary effects, such as surface currents and edge diffraction, which are not modeled by the flat plate model in (5).

For the water surface in Fig. 3b, the general shape matches well, but apparently the neglected side effects are stronger than for the metal plate. This could be due to the fact that the scattering model (6) assumes normal incidence, while in the measurement setup used for this paper there has been an offset of about $2°$ and on the other hand the model assumes $\lambda \ll \sqrt{A}$. Here, the conditions have been $\lambda \approx 0.1\sqrt{A}$.

4. Conclusion

In this paper it is shown that a UWB impulse radar system can be modeled in terms of impulse responses of the various elements in the transmission chain. In a stationary scenario, this leads to simulation results that coincide well with measurements. With a reference signal that matches the actual received pulse shape, a correlation receiver can achieve best performance. In realistic radar scenarios, however, deriving a perfectly matching reference pulse is usually not possible, especially if, for example, different objects such as different cars are to be detected. Thus, suboptimal methods for estimation of the reference signal have to be found and their impact on detection performance has to be analyzed.

The proposed simulation model will allow to analyze the influence of not perfectly matched reference pulses and thus contribute to the comparison of different signal processing approaches (e.g. energy detection versus correlation with an abstract reference pulse) which are trying to cope with the occuring effects.

(a) Validation using a metal plate with a surface area of $0.64\ \mathrm{m}^2$ at a distance of $1\ \mathrm{m}$ as target and both antennas in vertical polarization.

(b) Validation using a canister of water with surface area of $0.78\ \mathrm{m}^2$ at a distance of $1\ \mathrm{m}$ as target and both antennas in vertical polarization.

Figure 3: Validation of the proposed UWB impulse radar time domain simulator.

5. Acknowledgement

References

[1] Kurokawa, K.: *Power waves and the scattering matrix*. Microwave Theory and Techniques, IEEE Transactions on, 13(2):194 – 202, 1965, ISSN 0018-9480.

[2] Pancera, E.: *Strategies for Time Domain Characterization of UWB Components and Systems*. Phd thesis, Institut für Hochfrequenztechnik und Elektronik, Karlsruher Institut für Technologie, 2009.

[3] Kunisch, J.: *UWB radio channel modeling considerations*. In *Proc. ICEAA*, 2003.

[4] Sörgel, Werner and Werner Wiesbeck: *Influence of the antennas on the ultra-wideband transmission*. EURASIP J. Appl. Signal Process., pages 296 – 305, January 2005, ISSN 1110-8657.

[5] Baum, C.E.: *General properties of antennas*. Electromagnetic Compatibility, IEEE Transactions on, 44(1):18 –24, Feb 2002, ISSN 0018-9375.

[6] Knott, Eugene F., John F. Schaeffer, and Michael T. Tuley: *Radar Cross Section*. SciTech Publishing, Raleigh, NC, 2nd edition, 2004, ISBN 978-1-891121-25-8.

[7] Le Vine, D.: *The radar cross section of dielectric disks*. Antennas and Propagation, IEEE Transactions on, 32(1):6 – 12, Jan 1984, ISSN 0018-926X.

[8] Detlefsen, J. und U. Siart: *Grundlagen der Hochfrequenztechnik*. Oldenburg Verlag, München, Wien, 2. erweiterte Auflage, 2006, ISBN 978-3-486-57866-9.